Irrigation effects on the salinity of the Arba and Riguel Rivers (Spain): present diagnosis and expected evolution using geochemical models

J. Causapé · L. Auqué · Mª J. Gimeno · J. Mandado · D. Quílez · R. Aragüés

Abstract This work diagnoses the present salinity of the Riguel and Arba Rivers (Spain) and predicts its expected evolution using geochemical models applied to the modernization of the actual Bardenas I and the completion of irrigation in the Bardenas II irrigation districts. The results show a progressive increase in salinity (from 0.39 to 2.21 dS/m electrical conductivity) in the Riguel-Arba system, due to the cumulative collection of irrigation return flows and its progression towards more saline facies. The Bardenas I modernization, involving an increase in irrigation efficiency from 50 to 90%, will decrease the volume and salinity of the Riguel River by 30%. In contrast, irrigation of the new 24,000 ha Bardenas II land will increase the flow (12%) and salinity (21%) of the Arba River. Geochemical models may help in providing sensible estimates on the impact of irrigation on the salinity of the receiving water bodies.

Keywords Geology · Agriculture · Water · Salinity

Introduction

The quality of world water resources is being increasingly degraded as a consequence of its intensified anthropogenic exploitation. In particular, the expansion of irrigation in arid and semiarid areas and its inefficient use may lead to the salinization of the receiving water bodies, thus compromising the subsequent agricultural, urban and industrial uses of these waters (Tanji and Hanson 1990).

Several hydrosalinity balance studies performed in the most important irrigated areas of the Ebro River Basin have quantified the mass of salts exported in irrigation return flows. Thus, salt loading from La Violada (Monegros I), a flood-irrigated district with large amounts of gypsum in the soil, was between 17 and 20 Mg/ha/year (Faci and others 1985; Aragüés and others 1990; Isidoro 1999), whereas it was around 13 Mg/ha/year in two sprinkler-irrigated districts of Monegros II with saline-sodic lutites in the subsoil. In contrast, salt loading from the Arba basin (Bardenas irrigation district) was 6 Mg/ha/year (Basso 1994). Within this basin, the salt loading measured in different experimental sub-basins varied between 13.6–15.2 Mg/ha/year (Basso 1994; Lasanta and others 2002) in a flood-irrigated, salt-affected district, to 4.1 and 4.7 Mg/ha/year in two flood-irrigated, non-saline districts, and 3.4 Mg/ha/year in an sprinkler-irrigated, non saline district (Causapé 2002). As expected, these results show that off-site salinity pollution of irrigated agriculture basically depends on the amount of salts present in the soil and subsoil, and on the management and efficiency of the irrigation water.

Salt loading from irrigated agriculture in the Ebro Basin obviously affects the salinity levels and trends of the Ebro River. Thus, Quílez (1998) concluded from a Kendall analysis of the salinity of waters in the middle Ebro River (Zaragoza) that the total dissolved solids increased by 8.8 mg/l/year during the period 1960–1990. Extrapolating the salt loading exported from different irrigation districts of the Ebro Basin to the expected acreage of the basin to be transformed into irrigation, Machín and Navas (2001) estimated that the salinity of the Ebro River at Zaragoza will increase by around 15% (i.e., the average EC will increase from 1.2 to 1.4 dS/m, whereas the maximum EC will increase from 2.8 to 3.2 dS/m).

The minimization of these negative environmental effects requires an adequate planning and management of the irrigable areas based on an in-depth knowledge of their physical systems and the production factors. Proper simulation models may be used for simplifying the complex phenomena occurring in nature and predicting the

Received: 17 July 2003 / Accepted: 15 October 2003
Published online: 22 November 2003

J. Causapé (✉) · D. Quílez · R. Aragüés
Servicio de Investigación Agroalimentaria- Diputación General de Aragón (DGA) y Laboratorio de Agronomía y Medio Ambiente (DGA-CSIC), Apdo 727, 50080 Zaragoza, Spain
E-mail: jcausape@aragob.es
Tel.: +34-976-716324
Fax: +34-976-716335

L. Auqué · M.J. Gimeno · J. Mandado
Facultad de Ciencias Geológicas, Universidad de Zaragoza, Pedro Cerbuna 12, 50009 Zaragoza, Spain

changes of the studied systems under different hypothetical scenarios. Thus, a conceptual irrigation project hydrosalinity model has been used in the Ebro Basin to predict under various water management scenarios the volume and salinity of the irrigation return flows from La Violada (Aragüés 1990) and Monegros II (Quílez 1998) irrigation districts.

The objectives of this study are: (1) to analyze the spatial variability of dissolved salts in the Riguel and Arba Rivers and their relations with its catchment's geology; (2) to examine the basic processes involved in the salinization of the Riguel-Arba system using various geochemical models, and; (3) to use these models for estimating the salinization of the Riguel-Arba system under two hypothetical scenarios: the modernization of the currently irrigated Bardenas I district, and the transformation into irrigation of the Bardenas II irrigation district.

Materials and methods

The study area pertains to the Arba Basin, located in the middle Ebro Basin (North East Spain). Its geology consists largely of Quaternary glacis and alluvium lying over Tertiary materials that are the primary source for salts. The main rivers in the Arba Basin are Riguel, Arba de Luesia and Arba de Biel, which originate in the Santo Domingo Sierra and converge to form the Arba River, a tributary of the Ebro River (Fig. 1).

The climate of the area is characterized by hot summers and cold winters with large variations in daily temperatures. The average annual precipitation is 550 mm, although it decreases below 400 mm in the southern area, and the average annual reference evapotranspiration is close to 1,100 mm (IGME 1985). Spring and autumn are the more humid seasons, whereas summer and winter are the driest seasons. In consequence, crop water needs are not fully satisfied by precipitation, and irrigation is required between April and September to achieve maximum crop yields.

The Bardenas System, consisting of the Bardenas I and II irrigation districts, was initiated in 1958 with the construction of the Yesa Reservoir and the Bardenas Canal (Fig. 1). At present 52,600 ha are irrigated in Bardenas I, mainly by flooding, and 3,750 are sprinkler-irrigated in Bardenas II. Another 24,000 ha are still under transformation in Bardenas II (Confederación Hidrográfica del Ebro 2002). Most of the present irrigated land is drained by the Riguel and Arba Rivers and the newly irrigated land will be entirely drained by the Arba River. Thus, the quality of these rivers is or will be affected by the receiving irrigation return flows from these areas.

Four stratigraphic sections were selected from North to South in the Arba Basin (I-San Bartolomé, II-El Bayo,

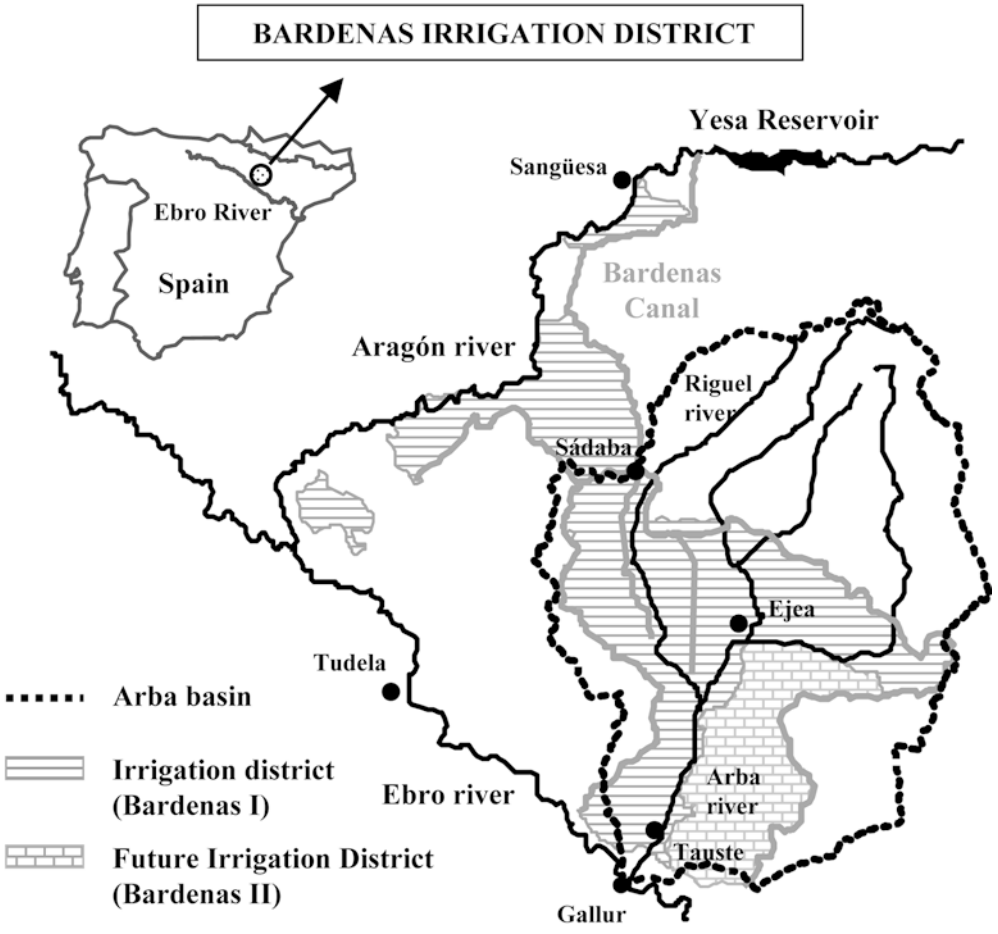

Fig. 1
Location of the Bardenas irrigation system with the Yesa Reservoir, the Bardenas Canal, the main rivers, and the current (Bardenas I) and future (Bardenas II) irrigation districts within the Arba basin

III-Castillo de Sora and IV-Tauste) (Fig. 2) for the analysis of their Tertiary geologic materials. A total of 21 rock samples representative of the different lithologies were collected for its chemical (SO_4^{2-},CO_3^{2-}, Ca^{2+}, Mg^{2+}, Na^+, K^+, H_2O, organic matter (OM) and insoluble residue or loss of ignition (LOI) after reaction with 0.8 N HCl at 50 °C for two hours) and mineralogical (X-ray diffraction and thin-section petrography) analysis. The rock samples were classified according to their chemical composition using a Cluster analysis. The data were standardized and the square Euclidean distance was used as a measurement of similitude. The Ward method was used to obtain the hierarchical associations (Hair and others 1999).

A total of 14 water sampling points were selected in the Riguel-Arba system to analyze the spatial variability of its chemical composition (Fig. 2). Eleven points were distributed along the Riguel (8 points) and the Arba (3 points) Rivers, from P1 in Riguel-Sádaba (start of the Bardenas irrigated area) to P11 in Arba-Gallur (point at which the Arba flows into the Ebro River). The other three points were located in the Bardenas Canal (BC), the Valareña Creek (V) and a spring of Bardenas I (S). On 27th June 2000, water samples were collected at each point and the temperature, pH and EC at 25 °C were determined in the field, whereas CO_3^{2-}, HCO_3^-, SO_4^{2-}, Cl^-, NO_3^-, Ca^{2+}, Mg^{2+}, Na^+ and K^+ were determined in the laboratory.

The values obtained in the analysis of the rock and water samples were processed using the geochemical computer codes WATEQ4F, NETPATH and PHREEQC developed by the US Geological Survey. WATEQ4F (Ball and Nordstrom 1991) is a thermodynamic model that performs speciation-solubility calculations, determines the saturation indexes with respect to minerals (calcite, dolomite, gypsum and halite) and gases (CO_2) and infers the tendency for minerals to dissolve or precipitate in a given environment. NETPATH (Plummer and others 1994) performs mass balance calculations and determines the amounts of reactive minerals and products which should dissolve or precipitate between selected initial and final points to cope with the measured ions at both points. This program was used to model the geochemical evolution of the water as it passes from irrigation (BC sample) to drainage (S sample) (i.e., evaporation and mineral dissolution-precipitation processes), and the incorporation of these drainage flows (S sample) to the Riguel waters at points P2 and P5, before the Valareña Creek outlet (i.e., water mixing and mineral dissolution-precipitation processes). PHREEQC (Parkhurst and Appelo 1999) is a reaction path code which determines the chemical composition of an aqueous solution and the amounts of minerals that will dissolve or precipitate under a set of hypothetical reactions and thermodynamic restrictions.

PHREEQC was used to validate the results obtained with NETPATH and to simulate two hypothetical scenarios. The first scenario analyzes the effect of the Bardenas I modernization, consisting of its complete transformation into

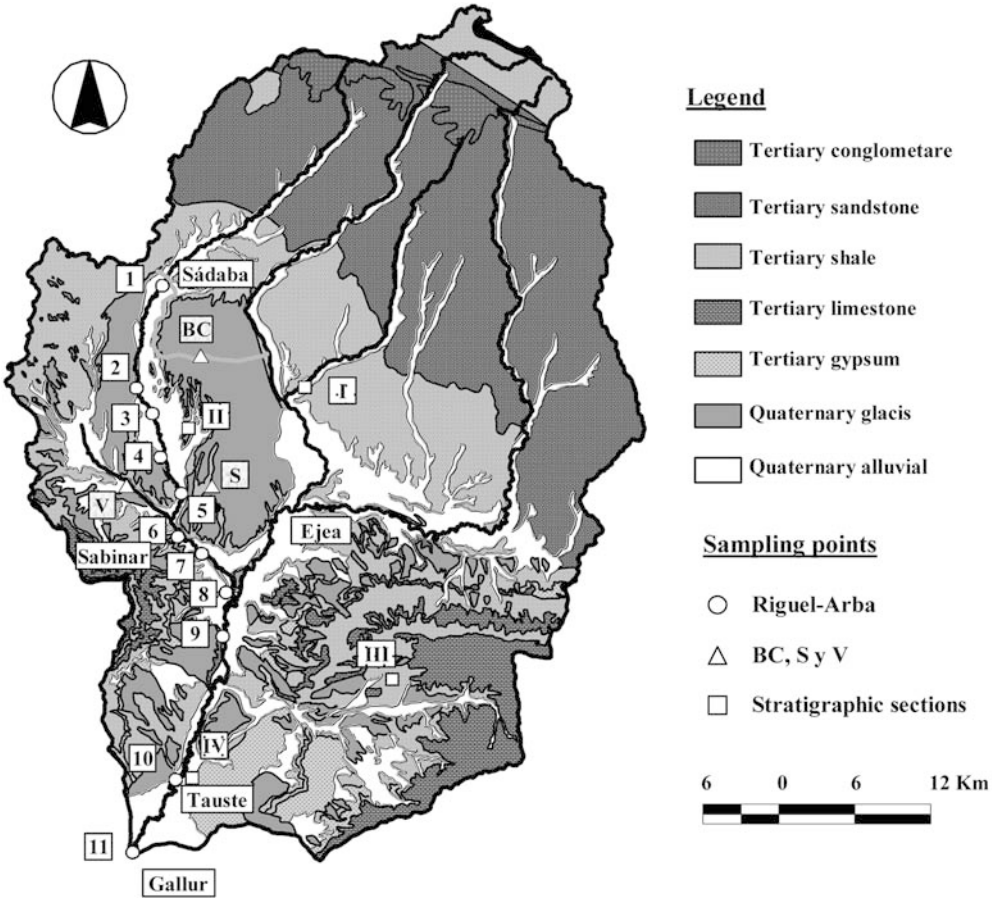

Fig. 2
Geology of the Arba basin and location of the water and geologic material sampling points

pressure irrigation systems, on the salinity of waters at the lower reaches of the Riguel River (P5). This sampling point was selected because it is located just before the Valareña outlet and because it collects the irrigation return flows of the glacis areas that are characterized by the chemical composition of the waters measured in the spring (S). The second scenario analyzes the effect of the complete transformation of Bardenas II into irrigation on the salinity of the Arba River waters at Tauste (P10). This sampling point was selected because it will collect all the Bardenas II irrigation return flows. These geochemical models allow us to approximate, under a set of specified hypothesis, the quality of drainage waters for the two given scenarios and the mixing ratio between the irrigation return flows and the river flows circulating through points P5 and P10.

Results and discussion

Geologic materials

Stratigraphic sections

Figure 3 shows the four stratigraphic sections and the position of the rock samples. The combined study of these sections indicates a sedimentation sequence along the North to South direction, from fluvial environments to lacustrine deposits. The northern area is a lutitic section with interbedded sandstone levels more abundant towards the top. These levels of sandstone are related to palaeo-channels with an erosive base, decreasing grain-classification and cross bedding (San Bartolomé). Towards the South the levels of sandstone become gradually less significant and banks of lacustrine limestones begin to appear (El Bayo). The southern area corresponds to central-basin facies consisting of alternating gypsum, clay and silt materials of brown and gray colors and with occasional intercalations of fine limestone layers associated with gypsum (Castillo de Sora and Tauste).

Chemical analyses

Based on the chemical composition of the 21 rock samples shown in Table 1, the cluster analysis classified them into three groups (Fig. 4). Group A (57% of the samples) includes all the samples located in the stratigraphic sections nearest to the source area (San Bartolomé and El Bayo), 55% of the samples in Castillo de Sora, and 37% of the samples in Tauste. Group B (29% of the samples) comprises 50% of the samples located in Castillo de Sora and Tauste, and group C includes two samples from Tauste and one from Castillo de Sora. A clear relationship can thus be established between the location of the samples from North to South and their inclusion in groups A to C. Group C has the

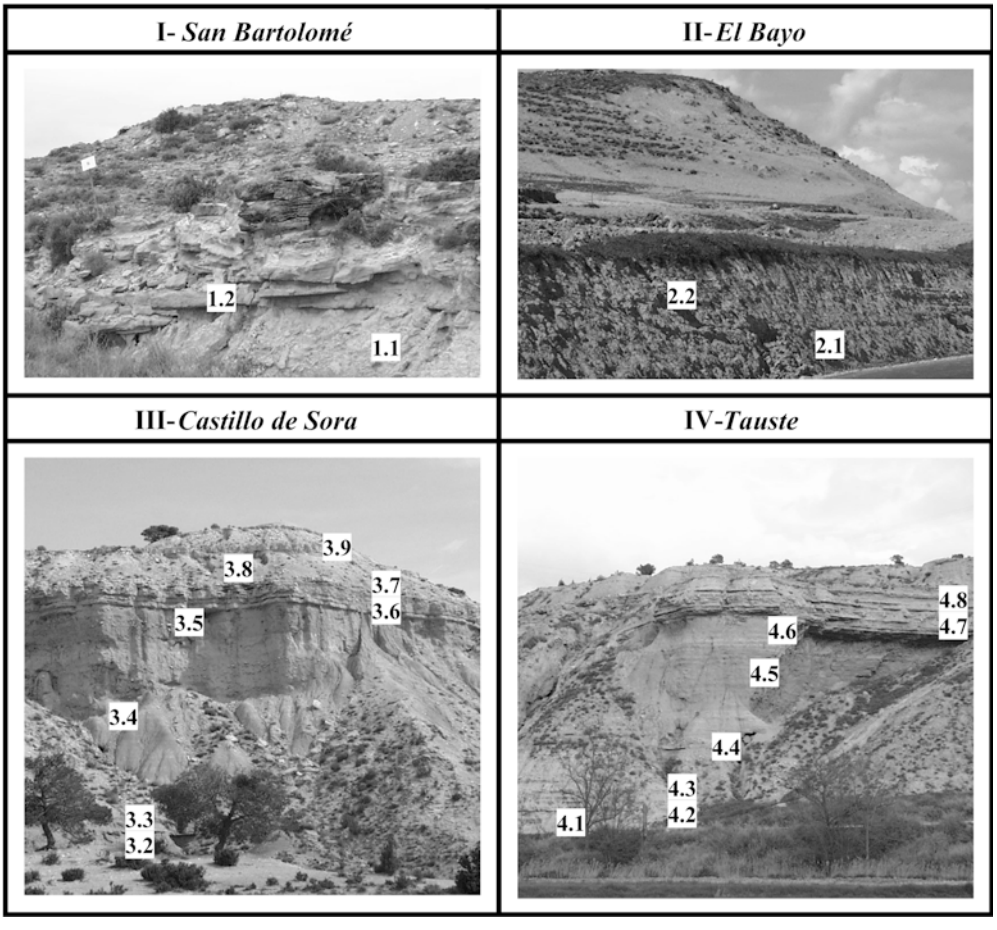

Fig. 3
Stratigraphic sections of San Bartolomé, El Bayo, Castillo de Sora and Tauste, and location of rock samples

Table 1
Chemical analyses of the 21 rock samples pertaining to the San Bartolomé, El Bayo, Castillo de Sora and Tauste stratigraphic sections

Sample	CO_3^{2-} (%)	SO_4^{2-} (%)	Ca^{2+} (%)	Mg^{2+} (%)	Na^{+} (%)	K^{+} (%)	H_2O (%)	OM[1] (%)	LOI[2] (%)	Total (%)
San Bartolomé										
1.1	14.44	1.51	10.24	0.18	0.32	0.09	1.57	4.35	66.10	98.80
1.2	26.89	0.96	16.36	0.16	0.10	0.04	0.34	0.88	51.04	96.77
El Bayo										
2.1	27.20	0.95	16.65	0.29	0.08	0.04	0.32	0.70	48.61	94.84
2.2	20.52	0.92	12.75	0.31	0.20	0.11	1.59	2.60	58.75	97.75
Castillo de Sora										
3.1	20.06	2.47	12.7	1.91	0.50	0.25	2.43	3.58	48.62	92.52
3.2	6.94	2.58	3.78	1.31	1.17	0.31	2.41	4.91	70.99	94.40
3.3	8.65	13.28	9.52	0.43	0.21	0.11	4.52	0.72	61.50	98.95
3.4	17.91	1.51	11.58	1.26	0.30	0.25	1.90	3.67	56.32	94.70
3.5	18.31	2.05	10.83	1.35	0.40	0.26	1.67	3.48	56.08	94.42
3.6	7.17	48.44	20.63	1.33	0.08	0.03	17.40	0.92	3.30	99.31
3.7	43.71	3.94	17.31	8.67	0.34	0.14	1.63	4.50	15.92	96.15
3.8	46.72	2.32	29.80	0.79	0.18	0.10	0.77	2.31	14.46	97.44
3.9	47.36	7.56	23.08	5.85	0.17	0.08	2.12	2.46	8.64	97.31
Tauste										
4.1	20.63	1.62	12.51	1.31	0.41	0.22	1.31	4.35	51.71	94.09
4.2	40.39	8.94	19.06	5.73	0.20	0.10	3.37	1.01	17.91	96.71
4.3	12.09	39.87	20.63	1.56	0.09	0.05	14.99	0.61	7.87	97.75
4.4	42.12	8.72	21.82	4.84	0.22	0.10	3.40	2.25	16.11	99.57
4.5	9.64	1.96	4.65	0.80	0.32	0.29	2.11	2.23	74.57	96.56
4.6	22.04	1.79	11.20	2.52	0.22	0.30	2.13	1.88	51.82	93.89
4.7	4.07	50.02	20.40	0.78	0.09	0.05	18.36	0.45	5.16	99.37
4.8	44.94	3.59	18.62	7.76	0.13	0.13	2.39	2.18	13.82	93.57

[1] Organic matter; [2] Loss of ignition

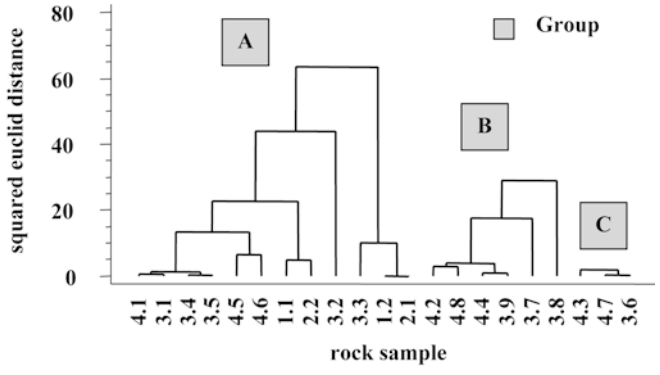

Fig. 4
Cluster analysis dendrogram based on the chemical composition (CO_3^{2-}, SO_4^{2-}, Ca^{2+}, Mg^{2+}, Na^{+}, K^{+}, H_2O, OM and IR) of the 21 rock samples

greatest similarity (distance <1), indicating the chemical similitude of the three samples in this group. Groups B and A have lower similarities, although they contain subgroups with similar chemical compositions.

The centroids of the chemical components measured in the 21 rock samples (Table 2) indicate that group A is characterized by siliceous minerals (LOI=58%), group B by carbonate minerals (CO_3^{2-}=44%) and group C by sulfate minerals (SO_4^{2-}=46%). The sampled rocks were very low in Na^{+} as compared to Ca^{2+} (Table 2), suggesting that the potential soil sodicity problems derived from the weathering of these rocks (i.e., loss of the soil's structural stability and Na toxicity in sensitive crops) should be negligible in the study area.
These results verify the parallelism between the chemical composition of the sampled rocks and the facies progradation in the Arba Basin, so that along the North to South direction there exists a consistent decrease in silicate minerals (group A), followed by an increase in carbonate minerals (group B) and finally by a sharp increase in sulfate minerals (group C).

Mineralogical and petrological analysis

The X-ray diffractograms (not shown) of the rock samples included in groups A and B detected a major

Table 2
Centroid values of the three groups discriminated by Cluster analysis

Group	CO_3^{2-} (%)	SO_4^{2-} (%)	Ca^{2+} (%)	Mg^{2+} (%)	Na^{+} (%)	K^{+} (%)	H_2O (%)	OM[1] (%)	LOI[2] (%)
A-siliceous	17.8	2.6	11.1	1.0	0.4	0.2	1.9	2.8	58.0
B-carbonated	44.2	5.9	21.6	5.6	0.2	0.1	2.3	2.5	14.5
C-sulphated	7.8	46.1	20.6	1.2	0.1	0.4	16.9	0.7	5.4

[1]Organic matter; [2]Loss of ignition

content of quartz (SiO_2) and calcite ($CaCO_3$) and a minor content of other carbonate minerals (ankerite ($Ca[Fe,Mg](CO_3)_2$), dolomite ($[Ca,Mg](CO_3)_2$), feldspars (albite, $NaAlSi_3O_8$ and anortite, $CaAl_2Si_2O_8$) and micas (muscovite, illite, chlorite, kaolinite). The A and B diffractograms differed in the proportion of the different minerals (quartz dominated group A, whereas calcite dominated group B). The diffractograms of group C indicated the dominance of gypsum ($CaSO_4{\cdot}2H_2O$) and a lower presence in basanite ($CaSO_4{\cdot}0.5H_2O$) and anhydrite ($CaSO_4$).

The petrographic study of the rock samples confirmed the presence of the minerals detected by X-ray diffraction, except basanite. The occurrence of this mineral in the diffractograms was attributed to gypsum dehydration during the grinding process.

Samples 1.2, 2.2 and 3.3 were classified as lithoarenites with dominating clasts of micritic calcium carbonate, quartz, feldspar and sparitic cement of calcite. The samples located in the southern area had rounded quartz minerals, less feldspars and a smaller grain size, revealing its greater transport distance.

The rest of samples from groups A and B were clayey or loamy and did not provide much information when studied under the microscope. Laminations marked by levels of small quartz clasts or fossils (bivalve) were frequently observed in these samples. Some samples had cracks occupied by gypsum that leaved residues at the edges of former veins.

The samples in group C (3.6, 4.3 and 4.7) comprised secondary gypsum, with microcrystalline textures in the interior zones and large crystals with inclusions of anhydrite in the exterior zones. The presence of biconvex morphologies in some samples would indicate a primary origin of lenticular gypsum, so that a formation characteristic of a subaerial sulfated precipitation process in playa-lake media may be inferred.

Chemical spatial variability of the Riguel-Arba River waters

Table 3 shows the chemical composition of the 14 water samples collected in the Riguel-Arba system. In general, the analyses were satisfactory, as indicated by the low error balances (absolute mean=4.6%). Its representation in a Piper diagram (Fig. 5) indicates that they evolved from a calcium-bicarbonated composition (water samples 1, 2, 3) with a low salinity (EC_1=0.39 dS/m), to a sodium-calcium chlorinated-sulfated-bicarbonated composition (samples 10 and 11) with a higher salinity (EC_{10}=2.21 dS/m). The Bardenas Canal (BC) and the spring (S) waters were calcium-bicarbonated, whereas the Valareña Creek (V) water was sodium-calcium chlorinated-sulfated-bicarbonated. The salinity of the BC water was very low (EC_{BC}=0.33 dS/m), as compared to that for S and V waters (EC_S=0.89 dS/m, CE_V=1.27 dS/m).

The spatial evolution of EC and ion concentrations in the Riguel-Arba system (Fig. 6) shows that, in general, they tended to increase along the direction of flow up to P10 (Tauste), decreasing thereafter (P11). HCO_3^- was the dominant anion in the first 30 km of the Riguel River, but Cl^- and SO_4^{2-} increased at P6 and were the dominant anions in Tauste (P10). The evolution of cations resembled that of anions: Na^+ paralleled Cl^- (halite source) and was the dominant cation in the final section of the Arba River, whereas Ca^{2+} (dominant in the first 30 km of the Riguel River) and Mg^{2+} responded to the variations in HCO_3^- and SO_4^{2-} (calcite, dolomite and gypsum sources). The higher Na^+ than Cl^- and the sharper increase in Mg^{2+} than in HCO_3^- in the lower reaches (>30 km) of the Arba River may be explained by the return flows dissolving sodium and magnesium sulfate minerals [such as thenardite (Na_2SO_4), mirabilite ($Na_2SO_4.10H_2O$) and epsomite ($MgSO_4.7H_2O$)] which, although not detected in the mineralogical analysis, are known to exist in the Zaragoza Formation of the lower Arba Basin (IGME 1980). Thus, the spatial evolution of the chemical com-

Table 3
Chemical analyses of the water samples collected on 27th June 2000 in the Riguel River (samples 1–8), Arba River (samples 9–11), Bardenas Canal (BC), Spring (S) and Valareña Creek (V)

Sample	T^{ra}	pH	CE	CO_3^2	HCO_3	SO_4^{2-}	Cl^-	NO_3^-	Ca^{2+}	Mg^{2+}	Na^+	K^+	Error balance[1] (%)
	(°C)		(dS/m)					(meq/l)					
1	19.5	8.2	0.39	0.04	3.20	0.74	0.46	0.08	2.76	0.69	0.77	0.03	−6.10
2	22.6	8.3	0.53	0.06	3.84	1.13	0.83	0.24	3.22	1.14	1.17	0.12	−7.83
3	21.6	8.2	0.61	0.00	4.08	1.17	0.87	0.29	3.56	1.22	1.25	0.11	−4.40
4	24.1	8.6	0.68	0.18	4.32	1.23	1.25	0.40	3.81	1.60	1.63	0.10	−3.27
5	21.4	8.0	0.77	0.00	4.38	1.87	1.68	0.52	4.16	1.54	2.23	0.10	−5.10
6	22.0	8.1	1.13	0.00	4.40	2.94	4.26	0.50	5.14	1.79	4.87	0.12	−1.46
7	23.7	8.0	1.10	0.00	4.44	2.62	4.09	0.52	5.20	1.76	4.59	0.13	0.08
8	21.7	8.1	1.13	0.02	4.58	2.34	3.55	0.58	5.33	1.68	3.83	0.12	−1.09
9	21.7	8.0	1.12	0.00	4.72	2.34	4.03	0.61	5.23	1.82	4.55	0.14	0.23
10	23.6	8.0	2.21	0.08	5.34	7.61	9.99	0.74	6.92	3.94	12.91	0.17	0.77
11	21.5	8.0	1.70	0.00	5.44	5.95	6.71	0.82	6.36	3.59	10.17	0.19	7.01
BC	16.8	8.0	0.33	0.00	3.07	0.65	0.31	0.08	2.64	0.49	0.48	0.03	−12.00
S	18.4	7.1	0.89	0.00	5.72	1.70	1.19	1.56	6.47	1.30	1.12	0.08	−12.64
V	22.2	8.1	1.27	0.00	4.08	3.77	4.82	0.53	5.66	1.84	6.00	0.13	3.16

[1] 100·[(cations-anions)/[(cations+anions)/2)]

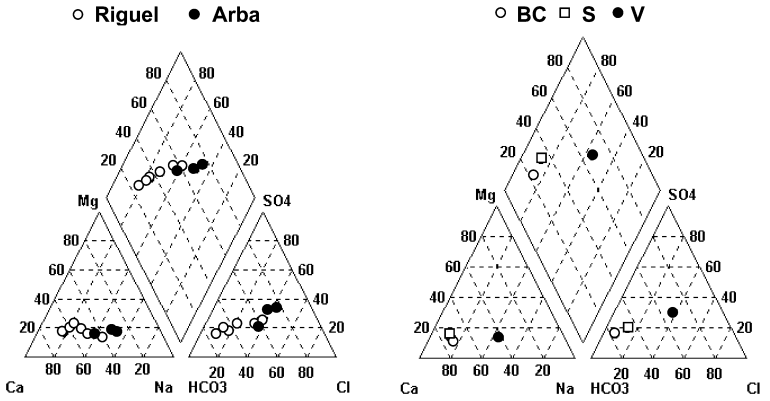

Fig. 5
Piper diagrams of the water samples collected on 27th June 2000 in the Riguel River (8 samples), Arba River (3 samples), Bardenas Canal (BC), Spring (S) and Valareña Creek (V)

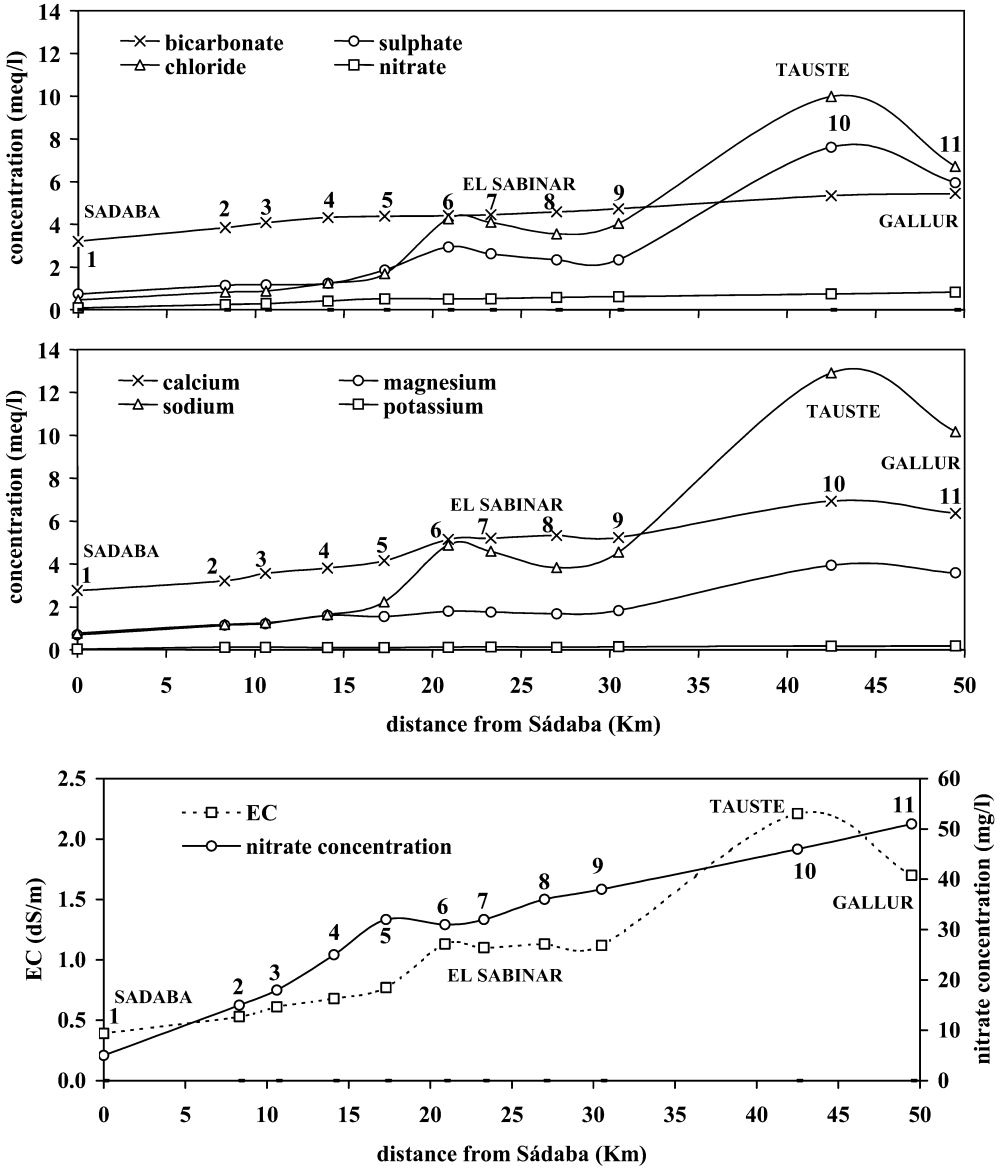

Fig. 6
Spatial evolution in the EC, anionic and cationic composition of the Riguel-Arba River waters from Sádaba (P1: Riguel River, start of the irrigated area) to Gallur (P11: Arba River, outlet to the Ebro River)

position of the waters in the Riguel-Arba system correspond to the spatial evolution of the chemical and mineralogical composition of the Tertiary geological materials (i.e., highly evaporitic minerals) present in the middle–lower Arba Basin.

As expected, the spatial evolution of EC in the Riguel-Arba system (Fig. 6) followed that of the ions. Thus, EC at Riguel-Sádaba (P1) was low (0.39 dS/m) and increased at a low rate of 0.02 dS/m per km up to P5, when it sharply increased (from 0.77 to 1.13 dS/m, equivalent to 0.1 dS/m

per km) due to the entrance of the more saline Valareña waters. The EC then remained constant for the next 10 km, after which it increased again rapidly (0.1 dS/m per km) reaching its maximum value of 2.21 dS/m at Arba-Tauste (P10) due to the previously indicated greater presence of evaporitic minerals. The Arba River in its final section drains low-salt waters from the Ebro River alluvium, and its EC at Gallur (P11) decreases to 1.70 dS/m.

Nitrate concentrations ($[NO_3^-]$) also increased in the Riguel-Arba flow direction, but its behavior was different to that of EC, revealing its agricultural origin as opposed to the main geological origin for salts (Fig. 6). Thus, $[NO_3^-]$ in the Riguel River was very low before the commencement of the irrigated area (5 mg/l at Sádaba-P1), but increased at a high rate of 1.6 mg/l per km in the section up to P5, when it stabilized due to the entrance of the low-nitrate Valareña waters (P6). Following this point, $[NO_3^-]$ steadily increased at a rate of 0.6 mg/l per km, reaching at Arba-Gallur (P11) the sanitary limit of 50 mg/l. The higher $[NO_3^-]$ rate increase in the Riguel section was due to the receiving drainage waters from extensive glacis with very permeable, shallow and stony soils (locally named "sasos"). The maize grown in these soils is heavily fertilized (400 kg N/ha) and is inefficiently flood-irrigated (irrigation efficiencies of around 50%), so that $[NO_3^-]$ in drainage ditches is very high (average of 55 mg/l in 28 ditches measured during the 1999–2000 hydrological year); Causapé 2002).

Geochemical characteristics of the Riguel-Arba River waters

The 11 water samples collected in the Riguel and Arba Rivers were supersaturated (SI>0) with respect to calcite and dolomite and undersaturated (SI<0) with respect to gypsum and halite (Fig. 7). The calcite and dolomite SI were independent of EC, whereas the gypsum and halite SI tended to increase with EC confirming the higher sulfate, chloride, calcium and sodium concentrations in the more saline waters.

The Bardenas Canal (BC) and spring (S) waters were in equilibrium with calcite and dolomite (SI=±0.5, which is within the uncertainty saturation value for these minerals). As expected, the spring water had a lower CO_2 partial pressure (log pCO_2=−1.62) than the rest of waters, which had log pCO_2 values between −3.24 and −2.55 (i.e., closer to the −3.5 value for the atmosphere).

Modelization of the irrigation return flows

The changes in the geochemistry of the irrigation water (CB) as it passes to drainage water (S) were simulated with NETPATH for two cases: without and with consideration of solution evapo-concentration due to crop's ET.

In the first case, where only the mineral's dissolution/precipitation was considered, the model estimates the amounts of calcite, dolomite, gypsum, halite and CO_2 that should dissolve in order to cope with the ions measured in BC and S (Table 4). The dissolution of 0.98 mmol/l of calcite calculated by NETPATH is apparently inconsistent due to the presence of petro-calcic horizons in the "saso" soils and the saturation status of both waters with respect to calcite (Fig. 7). However, since calcite solubility increases with CO_2, this dissolution was possible because of the CO_2 enrichment of the CB as it passes through the soil due to the presence of organic matter, root respiration and microbial decomposition. Thus, based on the chemical composition of the irrigation water (BC) and the pH of the spring water (S) (Table 3), PHREEQC predicted a partial pressure of CO_2 similar to that of the spring, and a negative calcite saturation index ($SI_{calcite}$=−0.46), which justifies the dissolution of this mineral. On the other hand, the gypsum (0.53 mmol/l) and halite (0.88 mmol/l) dissolutions calculated by NETPATH is less justified since these minerals are infrequent in the area of influence of the spring.

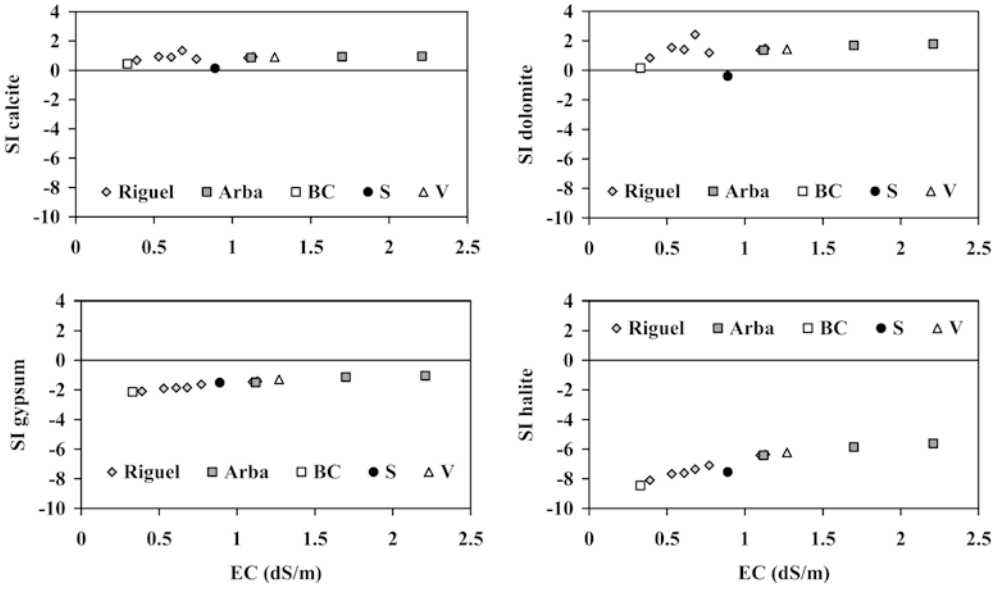

Fig. 7
Relationships between the calcite, dolomite, gypsum and halite saturation indexes (SI) and the EC measured in the water samples collected on 27th June 2000 in the Riguel River (8 samples), Arba River (3 samples), Bardenas Canal (BC), Spring (S) and Valareña Creek (V)

Table 4
Parameters and results of NETPATH simulating the changes in the geochemistry of the irrigation water (BC; initial solution) as it flows through the soil to conform the drainage water (S; final solution) without and with consideration of solution evapo-concentration due to crop's ET

NETPATH results without crop's evapo-concentration					
Parameters	Initial solution	Final solution	Constraints	Phases	
	BC	S	C, S, Cl, Ca, Mg	Calcite, dolomite, gypsum, halite, CO_2	
Results	Calcite	Dolomite	Gypsum	Halite	CO_2
	+0.98 (mmol/l)	+0.40 (mmol/l)	+0.53 (mmol/l)	+0.88 (mmol/l)	+1.78 (mmol/l)
NETPATH results with crop's evapo-concentration					
Parameters	Initial solution	Final solution	Constraints	Phases	
	BC	S	C, S, Cl, Ca, Mg	Calcite, dolomite, gypsum, halite	
Results	ET conc. factor	Calcite	Dolomite	Gypsum	Halite
	1.95	+0.14 (mmol/l)	+0.09 (mmol/l)	+0.11 (mmol/l)	+0.30 (mmol/l)

Table 5
Mixing proportions (%) of the Riguel River water at Sádaba (P1) and the spring water (S), and amounts of calcite, dolomite, gypsum and halite calculated with NETPATH to dissolve (+) or precipitate (-) to produce the Riguel waters at P2 and P5

Parameters					
Initial solutions P1 and S		Final solutions P2 and P5	Constraints C, S, Cl, Ca, Mg	Phases Calcite, dolomite, gypsum, halite	
Models					
	% S	Calcite (mmol/l)	Dolomite (mmol/l)	Gypsum (mmol/l)	Halite (mmol/l)
P1 to P2	18	−0.38	+0.17	+0.11	+0.24
P1 to P5	36	−0.68	+0.31	+0.39	+0.95

In the second case, where both the dissolution/precipitation of minerals and the ET evapo-concentration were considered, NETPATH assigned to the BC water an evaporation factor (Fc) of 1.95. Thus, the BC water will increase its measured EC of 0.33 to 0.64 dS/m due to Fc, and the remaining increase up to spring water EC of 0.89 dS/m would be assigned to mineral dissolution. In consequence, the amounts of minerals calculated to dissolve by NETPATH were much lower than in the first case (Table 4), although the patterns of dissolution were similar (i.e., greater dissolution of calcite than dolomite, and of halite than gypsum). The Fc value of 1.95 assigned by NETPATH is consistent with the average irrigation efficiency (IE) value of 0.50 obtained by Causapé (2002) for the study area, since under steady-state conditions Fc=1/IE. The consistency of these results was confirmed by PHREEQC. Thus, for a hypothetical Fc value of 1.95 applied to the BC water and the measured spring water pH of 7.1, the model predicted CO_2 partial pressure and calcite saturation index values similar to those obtained for the spring water (log pCO_2=−1.59 and $SI_{calcite}$=0.03).
It is therefore suggested that the spring water (S), representative of the irrigation return flows in the area, results from the evapoconcentration of the BC irrigation water by a factor of 1.95 plus a small dissolution of the minerals present in the geological materials of the northern half of Bardenas I (basically Quaternary alluvium and glacis developed on the sandstone-lutitic continental Tertiary materials).

Effects of irrigation return flows on the geochemistry of the Riguel and Arba River waters

Irrigation generates return flows which feed into the river courses through the drainage system. The water in the Riguel River comprises the mixing of the water flowing at the start of the irrigated area (P1, Riguel in Sádaba) and different proportions of the irrigation return flows in the area of influence, of which the spring (S) is a representative sample.
The models obtained for the passage of water from P1 to P2 and P5 (last point on the Riguel before the Valareña Creek outlet) show that the contribution of irrigation return flows (S) to the water flowing in the Riguel River increased progressively, from 18% at P2 to 36% at P5 (Table 5). During this passage, the models predict the precipitation of calcite due to the loss of CO_2 as the subterranean drainage flows emerge towards the surface. The amount of calcite precipitation as well as the dissolution of dolomite, gypsum and halite increased as the Riguel River advanced towards the central facies of its basin (more carbonated and evaporitic minerals) (Table 5).
Similarly, the model obtained for the passage of the Riguel River in Sádaba (P1) to the Arba River in Tauste (P10) followed the previously observed pattern (calcite precipitation and dolomite, gypsum and halite dissolution; Table 6) although the dissolved or precipitated masses were higher due to the greater distance between the sampling points and, particularly in the case of gypsum and halite, due to their greater presence in the lower Arba

Basin. The water in the Riguel-Arba system is gradually enriched with CO_2 due to the accumulation of drainage flows, which never reached equilibrium with the atmospheric CO_2.

Geochemical evolution of the Riguel and Arba River waters under two hypothetical scenarios

Scenario I: modernization of the Bardenas I irrigation district

This modernization implies a change in irrigation from the present flood-irrigation system to pressurized-irrigation systems. Based on the information gathered in the study area (Causapé 2002) and in other pressurized irrigation districts such as Monegros II (Tedeschi and others 2000), we set an average plot-irrigation efficiency (IE) of 90% for the modernized scenario I as compared to an IE of around 50% for the current situation. This increase in irrigation efficiency will imply a greater evapoconcentration of the infiltrated water and, thus, a potential change in the ion composition of drainage waters that was estimated with PHREEQC using an Fc=10 for the Bardenas Canal (BC) water.

The resulting solution will be undersaturated with respect to gypsum (SI_{gypsum}=−0.72) and halite (SI_{halite}=−6.56), although it will be closer to equilibrium than the sampled spring water S (SI_{gypsum}=−1.5, SI_{halite}=−7.5) due to the greater SO_4^{2-}, Cl^-, Ca^{2+} and Na^+ concentrations induced by the higher evapoconcentration. The higher HCO_3^- and Ca^{2+} concentrations will cause a greater calcite supersaturation ($SI_{calcite}$=2.01) which could eventually induce its precipitation and the corresponding development of petro-calcic horizons. These horizons could lead to the formation of perched water tables and, thus, to the salinization of soils due to groundwater rising and evapoconcentration at the soil surface. However, the effect of winter rainfalls, not considered in this analysis, could minimize this potential problem due to the re-dissolution of the precipitated calcite. After simulating the processes of evapoconcentration and dissolution-precipitation, the soil solution should be further balanced in terms of calcite and soil CO_2. This balance, performed using the pCO_2 of the spring water (log pCO_2=−1.6), produced a drainage water with a pH value of 7.1, similar to that of the spring water, whereas its TDS (1,281 mg/l) doubled that of the spring water (647 mg/l).

In the current scenario, we estimated previously that 36% of the water flowing in the Riguel River at P5 was drainage water (S). Thus, for each 100 volume-units of water at P5, 36 units were drainage water (S) and 64 units were water flowing in the Riguel River at P1. Since the IE in the current scenario is 50%, the 36 units of S water implied an application of irrigation water (BC) of 72 units (Fig. 8). Therefore, the P1: S mixing ratio at P5 will be 64:36=1.8. In the Bardenas I modernization scenario (i.e., increase in IE from 50 to 90%), the water demand for irrigation will theoretically decrease by up to 40%. However, we set a more realistic decrease of 30% since the modernization could lead to a decrease in the current crop's water stress (Causapé 2002) as well as a greater implantation of more water-demanding crops. Thus, in the modernized scenario 50 units of BC water will be applied (i.e., 30% less than the 72 units BC for the current scenario), 5 units of drainage water (S) will reach P5 (i.e., 90% of the 50 BC units), and 69 units will flow through P5 (i.e., the 64 units of water at P1 plus the 5 units of S water) (Fig. 8). Therefore, the P1: S mixing ratio at P5 will be 64:5=12.8. In summary, in the Bardenas I modernization scenario the drainage flows (S) will decrease by 86% (from 36 to 5 units of water), the water flowing through P5 will decrease by 31% (from 100 to 69 units) and the P1: S mixing ratio will increase by 7 (from 1.8 to 12.8).

This greater P1: S mixing ratio will cause a considerable reduction in the salinity of the flowing waters at P5, even though the drainage water TDS estimated in the modernized scenario was higher than the TDS in the current scenario. Thus, the TDS at P5 will decrease by 30% (from a measured value of 574 mg/l to an estimated value of 398 mg/l), with a concomitant reduction in ion's concentrations and gypsum and halite SI values (Table 7). However, this simulation overestimates the partial pressure of CO_2 and underestimates the pH and the calcite SI at P5. This is due to the loss of CO_2 as the subsurface drainage flows reach the atmosphere that was not taken into account in the simulation. Thus, a tendency towards equilibrium with the atmospheric CO_2 would reduce the partial pressure of CO_2 and would increase pH and $SI_{calcite}$, causing the precipitation of calcite and thus a reduction in the concentration of the HCO_3^- and Ca^{2+} ions.

Finally, it should be noted that the decrease in the salinity of the Riguel River due to an increase in the IE of the modernized Bardenas I irrigation district will be greater towards the south of the Arba Basin, where the dissolution of the evaporitic minerals will decrease due to the reduction in the volume of the irrigation return flows.

Table 6
Amounts of calcite, dolomite, gypsum, halite and CO_2 calculated with NETPATH to dissolve (+) or precipitate (-) for the path of the Riguel River waters at Sádaba (P1) to the Arba River waters at Tauste (P10)

Parameters				
Initial solution Sádaba (P1)	Final solution Tauste (P10)	Constraints C, S, Cl, Ca, Mg	Phases Calcite, dolomite, gypsum, halite, CO_2	
Model Calcite (mmol/l) −2.98	Dolomite (mmol/l) +1.62	Gypsum (mmol/l) +3.44	Halite (mmol/l) +9.54	CO_2 (mmol/l) +1.88

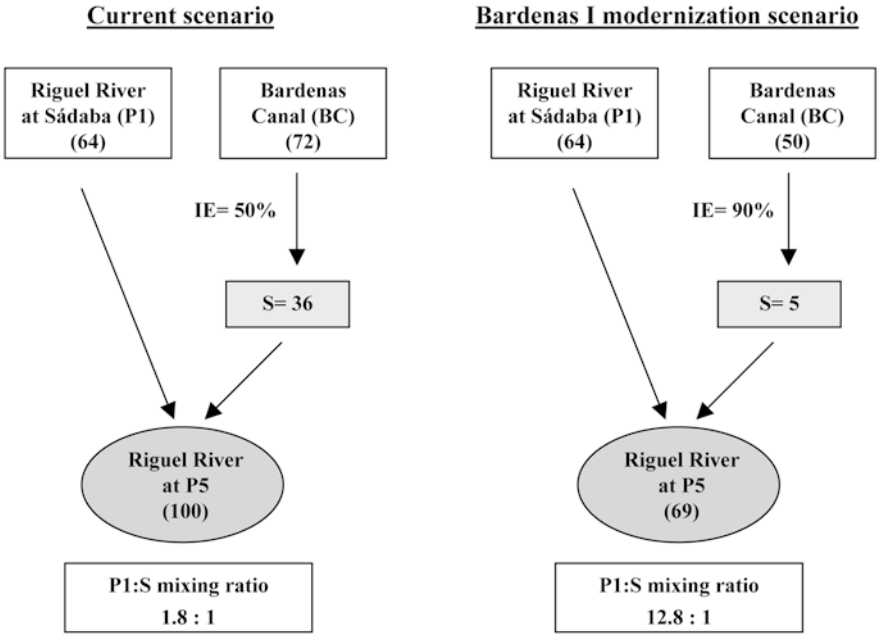

Fig. 8
Flow diagrams (in units of volume of water) of the irrigation return flows (S)-Riguel River (at P1 and P5) simulated systems for the current scenario (irrigation efficiency IE=50%) and the Bardenas I modernization scenario (irrigation efficiency IE=90%)

Table 7
Chemical characteristics of the Riguel River waters at P5 under the current scenario and the PHREEQC simulated scenario consisting of the Bardenas I modernization (i.e., a change in the plot irrigation efficiency from the actual value of 50% to a modernization value of 90%)

Riguel at P5	Current scenario	Bardenas I modernization
HCO_3^- (mg/l)	267	223
SO_4^{2-} (mg/l)	90	55
Cl^- (mg/l)	60	23
Ca^{2+} (mg/l)	83	57
Mg^{2+} (mg/l)	19	13
Na^+ (mg/l)	51	25
K^+ (mg/l)	3.9	1.9
TDS (mg/l)	574	398
pH	8.0	7.8
log pCO_2	−2.63	−2.56
SI calcite	0.76	0.39
SI gypsum	−1.63	−1.91
SI halite	−7.10	−7.81

Scenario II: total transformation into irrigation of the Bardenas II irrigation district

This transformation is projected for the remaining 24,000 ha in Bardenas II by means of pressurised irrigation systems. This new irrigated land will generate irrigation return flows that will be drained by the Arba River at Tauste (P10). Based on figures found in the pressurized Monegros II irrigation district (Tedeschi and others 2000), we set a volume of drainage water of 700 m^3/ha/year. Thus, the volume of drainage water reaching the Arba River from the new 24,000 ha irrigated in Bardenas II will be 16.8 Hm^3/year.

The average volume of water measured in the Arba River at P10 during the April to September irrigated season is 143 Hm^3 (Confederacion Hidrográfica del Ebro; years 1990 to 2000). Thus, this volume will increase by around 12% due to the new Bardenas II irrigation return flows. The estimated mixing ratio between the current average water flow at P10 and the hypothetical return flows from the new Bardenas II irrigated land will be 8.5.

The drainage flows from Bardenas II will be subject to evapoconcentration, the balance with calcite and CO_2 present in the soil, and the dissolution of evaporitic minerals (such as gypsum and halite) present in the geologic materials of this area (Fig. 2). Based on the average ion composition of 66 drainage water samples collected in Bardenas II (RENASA 1976), where the SI values were −0.7 for gypsum and −4.3 for halite, PHREEQC estimated a TDS value of 4,704 mg/l for the drainage waters of Bardenas II. This value is consistently higher than that found in Bardenas I as a result of the already noted greater presence of evaporitic minerals in Bardenas II and the higher evapoconcentration factor of the irrigation water due to its higher application efficiency.

The mixing of the present volume of water measured at P10 with the drainage waters from the new Bardenas II scenario will produce waters with a TDS of 1,862 mg/l, 21% higher than the actual TDS of 1,536 mg/l. The water will be supersaturated with respect to calcite, and the SI values for gypsum and halite will be higher than those for the current scenario (Table 8) as a consequence of the dissolution of these minerals by the irrigation return flows. Although these figures should be considered as a first approximation due to model constraints (i.e., other evaporitic minerals present in the area such as thenardite, mirabilite and epsomite were not considered in PHREEQC) and insufficient field data, they show that the impact of the new Bardenas II irrigated land on the salinity of the Arba River at Tauste (P10) could be moderate to high.

Table 8
Chemical characteristics of the Arba waters at P10 (Tauste) under the current scenario and the PHREEQC simulated scenario consisting in the completion of irrigation in Bardenas II

Arba at P10	Current scenario	Bardenas II irrigation	Arba Tauste	Current scenario	Bardenas II irrigation
HCO_3^- (mg/l)	326	320	TDS (mg/l)	1,536	1,862
SO_4^{2-} (mg/l)	365	416	pH	8.0	7.8
Cl^- (mg/l)	354	519	Log pCO_2	−2.5	−2.4
Ca^{2+} (mg/l)	138	149	SI calcite	0.95	0.75
Mg^{2+} (mg/l)	49	49	SI gypsum	−1.03	−0.99
Na^+ (mg/l)	297	401	SI halite	−5.61	−5.33
K^+ (mg/l)	6.7	7.0			

Conclusions

The Tertiary materials in the middle-lower Arba Basin show a sedimentation sequence along the North to South direction, from fluvial environments to lacustrine deposits, associated with a mineralogical sequence composed of siliceous (quartz, feldspar), carbonated (calcite, dolomite) and sulfated (gypsum) minerals.

The large irrigation return flows of the low-efficient Bardenas I irrigation district (Irrigation Efficiency, IE=50%), coupled to the facies progradation and the mineralogical sequence of the geologic materials, determine the spatial variability in the salinity and chemical composition of the Riguel-Arba River waters. Thus, these waters evolve from a low salinity (EC=0.39 dS/m), calcium-bicarbonated composition at the beginning of the Riguel River (P1) to a relatively high salinity (EC=2.21 dS/m), sodium-calcium-chlorinated-sulfated-bicarbonated composition at the end of the Arba River (P10). These waters are slightly supersaturated (SI>0) in calcite and dolomite and clearly undersaturated (SI<<0) in gypsum and halite. However, the SI values of these two minerals increase along the direction of flow, reflecting its progressive dissolution in line with the greater presence of evaporitic minerals in the lower Arba Basin.

The Bardenas I modernization scenario (i.e., an increase in IE from the current 50 to 90%) will cause a 30% decrease in the demand of irrigation water, a 86% decrease in the volume of irrigation return flows, and a 31% decrease in the flow of the Riguel River at P5. In spite of the two-fold increase in the TDS of irrigation return flows due to the greater evapoconcentration of the irrigation water, the salinity of the Riguel waters at P5 will decrease by around 30% as a consequence of the lower volumes of irrigation return flows. We therefore concluded that the modernization of the Bardenas I irrigation district will save good-quality water in the Yesa Reservoir and will significantly improve the quality (salinity) of the Riguel-Arba River waters at the expense of a decrease in the flows reaching the Ebro River.

The scenario of the full transformation into irrigation of the 24,000 ha Bardenas II irrigation district will increase the demand of irrigation water by about 168 Hm^3 (35% of the capacity of the Yesa Reservoir). The presence of evaporitic minerals in the lower Arba Basin will cause irrigation return flows with salinity values close to 5,000 mg/l. In consequence, the irrigation return flows of the new Bardenas II irrigated land will increase the flow of the Arba River at Tauste (P10) by 12% and its salinity by 21% (from the actual value of 1,536 mg/l to an estimated value of 1,862 mg/l). This salinity increase is subject to further analysis based on subsequent studies to be undertaken in the study area.

Acknowledgements This work was supported by a grant from Consejo Superior de Investigaciones Científicas of Diputación General de Aragón (Spain). We thank Laboratorio para la Calidad de la Edificación (DGA), Confederación Hidrográfica del Ebro and Enrique Oliver and Pilar Iglesias for his support.

References

Aragüés R, Tanji KK, Quílez D, Faci J (1990). Conceptual irrigation project hydrosalinity model. Agricultural salinity assessment and management. ASCE Manuals and Reports on Engineering Practice No 71

Ball JW, Nordstrom DK (1991) User's manual for WATEQ4F, with revised thermodynamic database and test cases for calculating speciation of major, trace and redox elements in natural waters. USGS Open File Report, pp 91–183

Basso L, (1994) Los retornos salinos del polígono de riego Bardenas I y su contribución a la salinización de los ríos Arba y Riguel. Tesis Doctoral, Universidad de Zaragoza, Facultad de Filosofía y Letras, Departamento de Geografía y Ordenación del Territorio, 244 pp

Causapé J (2002) Repercusiones medioambientales de la agricultura sobre los recursos hídricos de la Comunidad de Regantes nº V de Bardenas (Zaragoza). Tesis Doctoral, Universidad de Zaragoza, Departamento de Ciencias de la Tierra, 153 pp. (Available in http://www.cervantesvirtual.com)

Confederación Hidrográfica del Ebro (2002) Nuevos regadíos de Aragón. Available in http://www.chebro.es

Faci J, Aragüés R, Alberto F, Quílez D, Machín J, Arrúe JL (1985) Water and salt balance in an irrigated area of the Ebro River Basin (Spain). Irrigation Sci 6:29–37

Hair J, Anderson R, Tatham R, Black W (1999) Análisis Multivariante. Prentice Hall Iberia, Madrid, 832 pp

IGME (1980) Mapa Geológico de España 1:200,000, Hoja 32, Zaragoza. Ministerio de Industria y Energía, Instituto Geológico y Minero de España, Madrid, 33 pp

IGME (1985) Investigación de los recursos hidraúlicos totales de la cuenca del Arba. Ministerio de Industria y Energía, Instituto Geológico y Minero de España, Madrid

Isidoro D (1999) Impacto del regadío sobre la calidad de las aguas del barranco de La Violada (Huesca): salinidad y nitratos. Tesis Doctoral, Universidad de Lérida, Escuela Técnica Superior de Ingeniería Agraria, Departamento de Medio Ambiente y Ciencias del Suelo, 267 pp

Lasanta T, Mosch W, Pérez-Rontomé MC, Navas A, Machín J, Maestro M (2002) Effects of irrigation on water salinization in semi-arid environments: a case study in Las Bardenas, Central Ebro Depression, Spain. In: García-Ruíz JM, Jones A, Arnáez J (eds) Environmental change and water sustainability. Instituto Pirenaico de Ecología, Zaragoza, Spain, pp 198–218

Machín J, Navas A (2001) Salinidad de las aguas superficiales. Efectos sobre el medio ambiente. "Herramienta informática para el análisis de los riesgos de salinización de las aguas superficiales tras la implantación de nuevos regadíos". Departamento de Edafología, Estación Experimental de Aula Dei-CSIC, Zaragoza, Spain, 110 pp

Parkhurst DL, Appelo CA (1999) User's guide to PHREEQC, a computer program for speciation, reaction-path, advective-transport, and inverse geochemical calculations. Water Resources Investigation Report 99–4259, USGS, 312 pp

Plummer LN, Prestemon EC, Parkhurst DL (1994) An interactive code (NETPATH) for modelling NET geochemical reactions along a flow PATH-version 2.0. USGS Report 95–4169

Quílez D (1998) La salinidad en las aguas superficiales de la cuenca del Ebro. Análisis del impacto potencial del regadío de Monegros II. Tesis Doctoral, Universidad de Lleida, Escuela Técnica superior de Ingeniería agraria, Departamento de Medio Ambiente y Ciencias del Suelo, Spain, 352 pp

RENASA (1976) Estudio detallado de suelos de los sectores I al XX- 2ª Parte de la zona regable de las Bardenas (Zaragoza). Recursos Naturales SA, Spain, 118 pp

Tanji KK, Hanson BR (1990) Drainage and return flows in relation to irrigation management. In: BA Stewart and DR Nielsen (eds) Irrigation of agricultural crops. Agronomy No 30, Am Soc Agronomy, Madison, Wisconsin, pp 1057–1088

Tedeschi A, Beltrán A, Aragüés R (2000) Irrigation management and hydrosalinity balance in a semi-arid area of the middle Ebro River basin (Spain). Agr Water Manage 49:31–50